Current Biology

Flies Regulate Wing Motion via Active Control of a Dual-Function Gyroscope

Highlights

- Flies possess specialized hindwings called halteres that function in flight control

- Halteres oscillate during flight, sending phasic sensory signals to flight muscles

- Halteres are equipped with tiny muscles that receive visual input during flight

- By activating the haltere muscles, flies can adjust wing motion to steer

Authors

Bradley H. Dickerson,
Alysha M. de Souza, Ainul Huda,
Michael H. Dickinson

Correspondence

flyman@caltech.edu

In Brief

Flies possess specialized hindwings called halteres, which function both as a gyroscope and as a clock to provide phasic drive to the flight motor. Using various genetic tools, Dickerson et al. show that flies use tiny muscles at the base of the haltere to adjust the activity of its sensory neurons and thus regulate the function of wing muscles.

CellPress

Flies Regulate Wing Motion via Active Control of a Dual-Function Gyroscope

Bradley H. Dickerson,[1,2] Alysha M. de Souza,[1] Ainul Huda,[1] and Michael H. Dickinson[1,3,*]
[1]Division of Biology and Biological Engineering, California Institute of Technology, Pasadena, CA 91125, USA
[2]Present address: Department of Biology, University of North Carolina at Chapel Hill, Chapel Hill, NC 27599, USA
[3]Lead Contact
*Correspondence: flyman@caltech.edu
https://doi.org/10.1016/j.cub.2019.08.065

SUMMARY

Flies execute their remarkable aerial maneuvers using a set of wing steering muscles, which are activated at specific phases of the stroke cycle [1–3]. The activation phase of these muscles—which determines their biomechanical output [4–6]—arises via feedback from mechanoreceptors at the base of the wings and structures unique to flies called halteres [7–9]. Evolved from the hindwings, the tiny halteres oscillate at the same frequency as the wings, although they serve no aerodynamic function [10] and are thought to act as gyroscopes [10–15]. Like the wings, halteres possess minute control muscles whose activity is modified by descending visual input [16], raising the possibility that flies control wing motion by adjusting the motor output of their halteres, although this hypothesis has never been directly tested. Here, using genetic techniques possible in *Drosophila melanogaster*, we tested the hypothesis that visual input during flight modulates haltere muscle activity and that this, in turn, alters the mechanosensory feedback that regulates the wing steering muscles. Our results suggest that rather than acting solely as a gyroscope to detect body rotation, halteres also function as an adjustable clock to set the spike timing of wing motor neurons, a specialized capability that evolved from the generic flight circuitry of their four-winged ancestors. In addition to demonstrating how the efferent control loop of a sensory structure regulates wing motion, our results provide insight into the selective scenario that gave rise to the evolution of halteres.

RESULTS AND DISCUSSION

The wings and halteres of flies are serially homologous structures that share many morphological features [10, 17]. For example, both are equipped with arrays of mechanosensory organs called campaniform sensilla, which encode strains within the cuticle as the wings and halteres oscillate back and forth during flight. The campaniform sensilla on the wing encode the aerodynamic and inertial forces produced on the wing as it flaps back and forth, whereas specialized campaniforms on the base of the haltere are thought to be sensitive to Coriolis forces induced by body rotation during flight, thus allowing the structure to function as a gyroscope [10, 11]. In addition to the campaniform sensilla, the wing and the haltere are also equipped with serially homologous sets of tiny control muscles [16, 18–20]. Whereas the role of the wing control muscles is quite clear—they regulate the production of aerodynamic forces during flight—the function of the halteres control muscles remains enigmatic. Twenty years ago, Chan and coworkers [16] reported that the activity of several haltere control muscles were regulated by descending visual input in quiescent, non-flying blowflies. Based on these results, they proposed the "control-loop hypothesis," in which descending commands from the visual system might regulate flight by effectively mimicking the compensatory steering reflexes that are normally triggered by the body rotation sensed by the haltere. In their scheme, descending commands generate virtual perturbations that activate steering maneuvers via strong monosynaptic connections between haltere campaniforms and wing steering motor neurons [8, 16]. Up until now, however, the control loop hypothesis has remained untested. In particular, it is not known whether changes in the activity of haltere steering muscles can actually alter the activity of wing steering muscles in flying flies.

To directly evaluate the role of the haltere motor system in flight control, we first investigated whether their tiny steering muscles are modulated by descending visual input during flight. *Drosophila* possesses seven haltere steering muscles (Figure 1A), fewer than in some larger fly species [16, 18–20]. In addition to the control muscles, a much larger asynchronous muscle (hDVM) also inserts at the base of the haltere, which plays an important role in oscillating the structure during flight [21]. We used the GAL4-UAS system to express the genetically encoded calcium indicator GCaMP6f in a driver line (*R22H05-GAL4*) that targets all of the haltere steering muscles and imaged their activity directly through the cuticle with an epifluorescent microscope during tethered flight (Figure 1B). The tiny haltere control muscles are tightly packed, and thus, it is not possible to segment them all individually, as can be done with the much larger wing muscles [22]. We could, however, distinguish the activity between two clustered anatomical groups: the anterior haltere basalar muscles (hB1 and hB2) and the more posterior haltere axillary muscles (hI1, hI2, hIII1, hIII2, and hIII3).

We presented flies with a series of wide-field rotational stimuli consisting of random starfields about the sagittal (yaw-roll) and
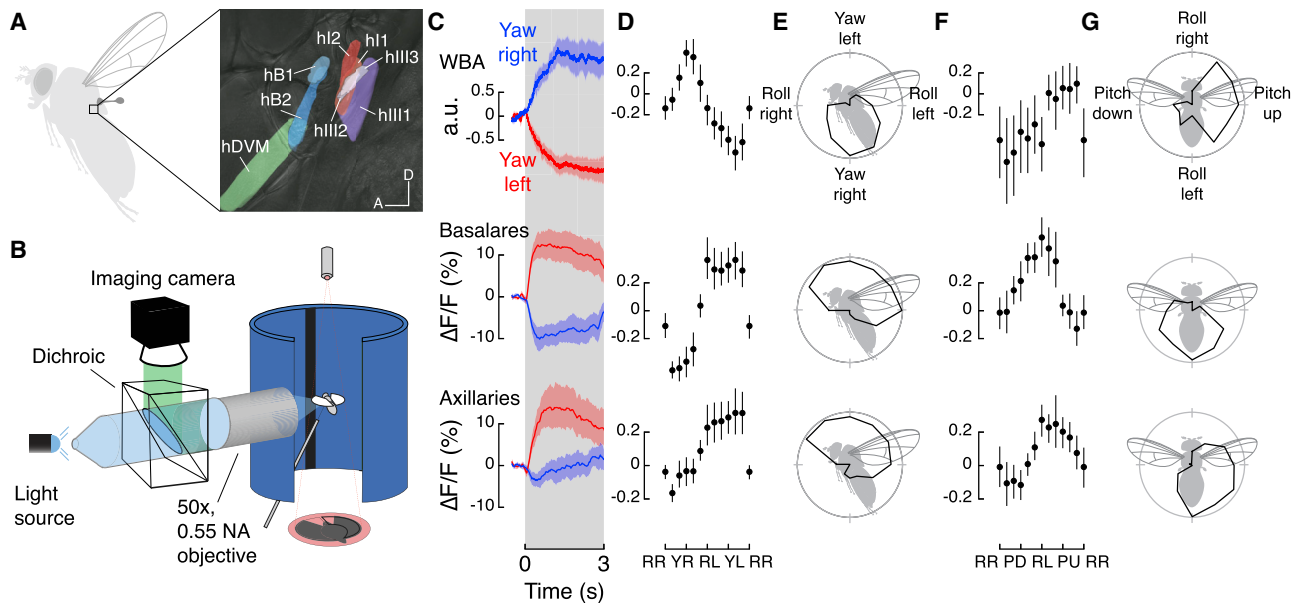
Figure 1. Haltere Muscle Activity Is Modulated by Visual Input and Tuned to the Cardinal Axes of Rotation

(A) The halteres of *Drosophila* possess one indirect asynchronous power muscle (hDVM) and seven direct synchronous steering muscles that can be divided into two groups: the basalares (hB1 and hB2) and the axillaries (hI1, hI2, hIII1, hIII2, and hIII3).

(B) Schematic of setup used to simultaneously image muscle activity and track wing motion in response to visual stimuli.

(C) Wingbeat amplitude (WBA) responses and fluorescence changes in the basalar and axillary muscles during 3-s presentations of wide-field yaw motion to the left (red) and right (blue). Data shown represent mean ± 95% confidence intervals (CIs). n = 19 flies.

(D) Tuning curves to a series of rotations (in 30° increments) about the yaw-roll axis constructed from the normalized mean integrated value during the stimulus epoch. RL, roll left; RR, roll right; YL, yaw left; YR, yaw right. Roll right is plotted twice to emphasize the cyclical nature of the data. Values in individual trails were calculated from the integral of the response curve during stimulus presentation. Data shown represent mean ± 95% confidence intervals (CIs). n = 15 flies.

(E) Polar projection of tuning curves shown in (D).

(F) As in (D) but for rotations about the pitch-roll axis (n = 15). RR, roll right; PD, pitch down; RL, roll left; PU, pitch up.

(G) Polar projection of tuning curves shown in (F).

See also Figure S1 and Video S1.

coronal (pitch-roll) planes while simultaneously tracking wing-stroke amplitude with an optical sensor. As indicated by changes in the GCaMP6f signal, both sets of muscles become active during flight and are modulated by the presentation of wide-field visual motion (Figure 1C; Video S1). The visual stimuli also elicited changes in wingstroke amplitude, consistent with the well-studied optomotor response [23] (Figures 1C–1G, top). The signals from both muscle groups are tuned roughly sinusoidally to the rotational axis of visual motion in the sagittal plane, with peak activity elicited by a yaw stimulus toward the side ipsilateral to the imaged haltere muscles (yaw left; Figures 1D, 1E, and S1A). For visual rotations about the coronal plane, both muscle groups exhibited a peak in activity during presentation of visual roll stimuli moving downward toward the ipsilateral side (roll left; Figures 1F, 1G, and S1B). We acknowledge that the responses we record represent the composite activity within each of the two muscle groups and that the tuning of individual muscles might differ from the summed activity of each cluster. Nevertheless, the experiments demonstrate that the activity of haltere control muscles is regulated in response to visual motion signals in flying *Drosophila*, an observation that had only been observed previously in quiescent blowflies (*Calliphora*) [16]. Furthermore, the composite tuning responses we measured are similar to that of an identified descending neuron that innervates the haltere motor neuropil (descending neuron of

the horizontal system [DNHS]), which is also maximally sensitive to ipsilateral roll [24]. However, we have no direct evidence that DNHS is responsible and many other descending neurons might be involved.

One possible function for visually mediated control of the haltere muscles is that the haltere efferent system alters the firing pattern of the campaniform sensilla at the base of the haltere (Figure 2A). To test this hypothesis, we recorded the activity of haltere afferent axon terminals during flight while presenting visual motion. The haltere afferents send collateral projections into the subesophageal zone (SEZ) of the brain (Figures 2B and 2C), where it is possible to image activity in tethered flying flies while keeping the thorax intact. These cells are serially homologous to campaniform afferents on the wing [25] (Figure 2D), which also send collaterals to the SEZ (Figures 2E and 2F). We used the driver line *DB331-GAL4* to express GCaMP6f in the SEZ terminals of the haltere and used 2-photon microscopy to record afferent activity during flight [26] (Figure 2G). This driver line labels the distal wing campaniform sensilla embedded along the wing blade; however, these campaniforms are a distinct population from those at the base and do not project to the SEZ [27]. As with our analysis of the haltere muscles, we presented flying flies with rotation of starfield patterns about the cardinal axes while simultaneously recording changes in wingstroke amplitude. Whereas some fraction of
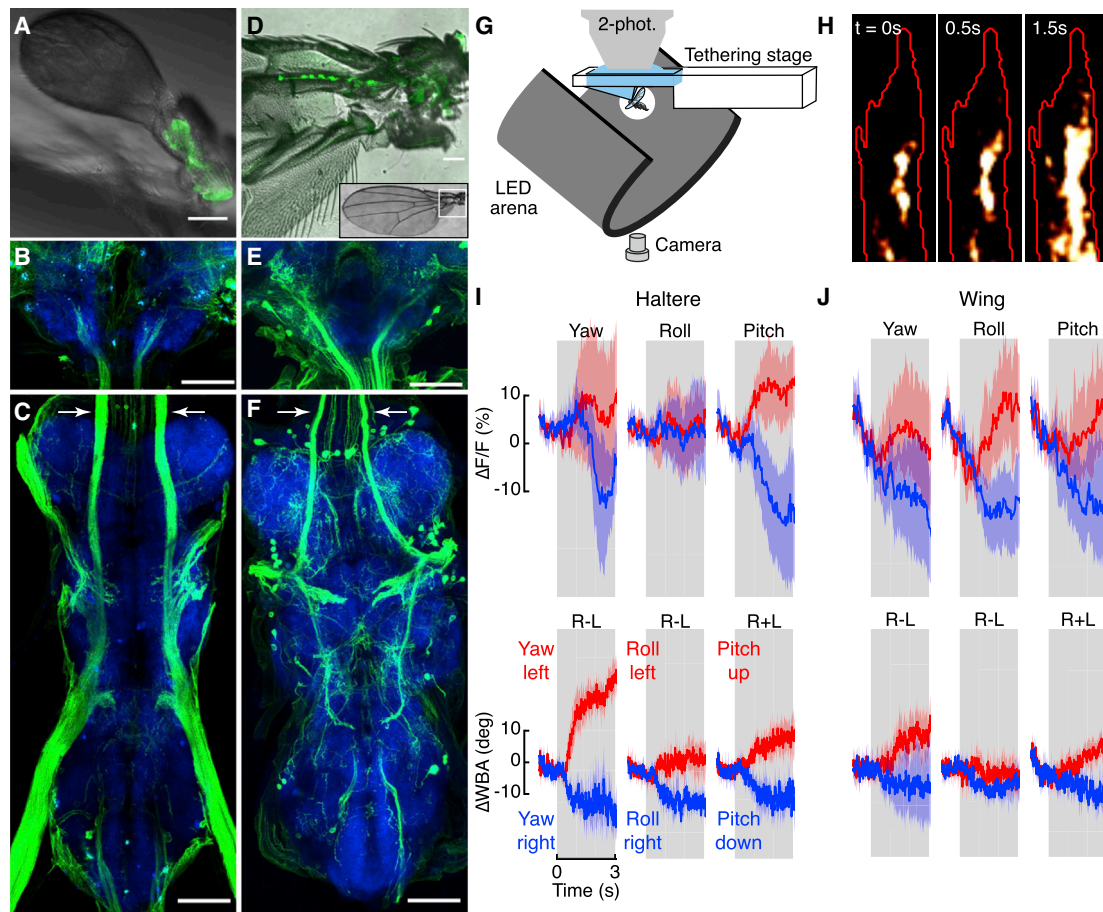
Figure 2. Wing and Haltere Afferent Activity Is Modulated by Visual Input

(A–C) Light micrographs of the peripheral (A) and central (B, SEZ; C, VNC) locations of haltere campaniform afferents labeled by crossing *UAS-GFP* with *DB331-GAL4*. Scale bars: 50 μm. Images in (B) and (C) are maximum intensity projections; blue shows nc82 staining. Arrows in (C) indicate the ascending tracts of haltere campaniform afferents. Image in (B) shows terminal projections of haltere campaniforms in the SEZ.

(D–F) As in (A)–(C) but showing peripheral (D) and central (E and F) locations of wing campaniform sensilla labeled by crossing *UAS-GFP* with *R12C07-GAL4*. Arrows in (F) indicate the ascending tracts of the proximal wing campaniform afferents. Image in (E) shows terminal projections of proximal wing campaniforms in the SEZ. Note that both driver lines also label off-target interneurons in the brain.

(G) Schematic of setup used to image haltere or wing campaniform activity during tethered flight.

(H) Maximum intensity projection of the right haltere afferent axon terminals for a single experiment with region of interest outlined in red.

(I and J) Changes in fluorescence (top) and wingbeat amplitude (WBA) (bottom) for the haltere (I) and wing (J) afferents in response to bilateral presentations of wide-field rotations about the cardinal axes. n = 6 flies each. Data shown represent mean ± 95% CI.

See also Videos S2 and S3.

the haltere afferents were tonically active during flight, we also observed a modulation in activity in response to the presentation of visual motion (Figures 2H and 2I; Video S2). To gain further insight into the organization of the entire flight control system, we used the *R12C07-GAL4* line to drive GCaMP6f expression in the campaniform afferents at the base of the wing [17] (Figures 2D–2F; Video S3). Like the haltere cells, we found that the wing afferents are tonically active during flight and modulated during visual motion (Figure 2J). Whereas the wing terminals responded to visual motion about all three rotational axes, the haltere axon terminals responded to yaw and pitch, but not roll (Figures 2I and 2J). Because we cannot resolve individual cells, we cannot rule out the possibility that some responses are masked by cases in which some cells increase in activity and others decrease.

Previous physiological work on wing and haltere campaniform neurons indicates that these cells fire single, phase-locked action potentials in each cycle of oscillatory motion across a broad range of frequencies [28, 29]. Furthermore, increased strain due to wing bending leads to recruitment of additional sensilla at different phases of the stimulus cycle [28]. Due to these features of physiology, we interpret increases in the GCaMP signal as reporting the recruitment of additional cells within the population and not as changes in the firing rate of active cells. This interpretation that the wing and haltere campaniforms encode kinematics via a population code rather than a spike frequency code is consistent with previous studies [10, 28, 30]. The modulation in activity of wing campaniforms is expected, because visual motion elicits changes in wing kinematics and thus aerodynamic and inertial forces, which in turn are likely to
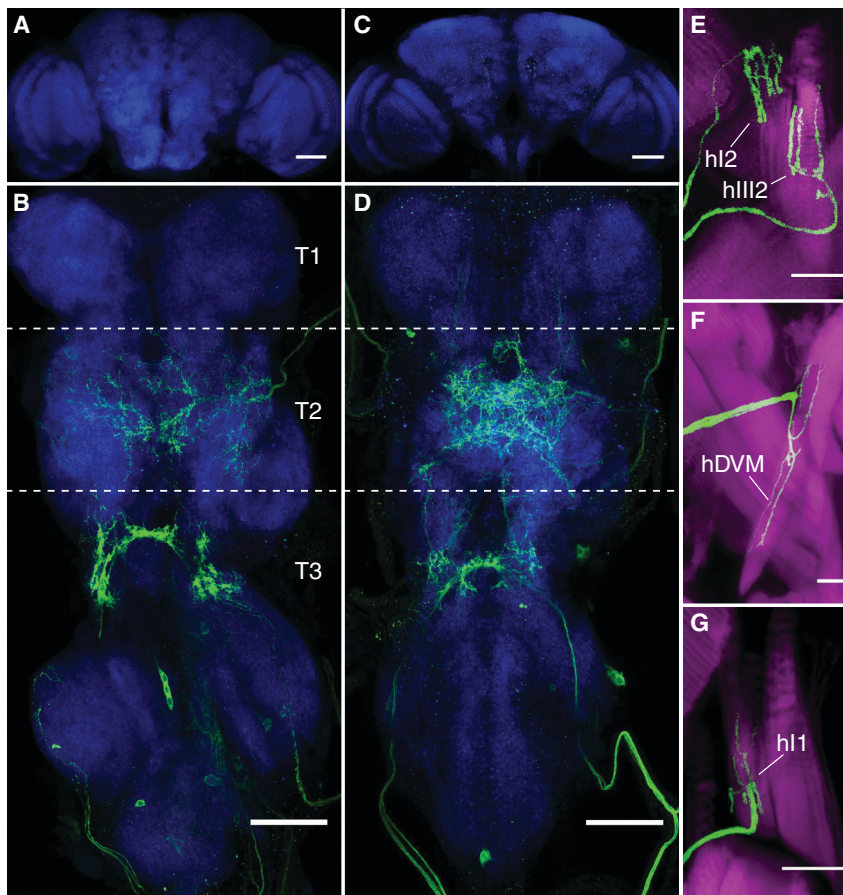
Figure 3. Haltere Steering Muscle Motor Neurons Labeled by Split-GAL4 Lines

(A and B) Maximum intensity projections of the brain (A) and VNC (B) expressing GFP driven by *SS36076-GAL4*.

(C and D) Maximum intensity projections of GFP driven by *SS41075-GAL4* in brain (C) and VNC (D). The haltere motor neurons of both driver lines are found in the metathoracic segment (T3) of the VNC. Blue shows nc82 staining.

(E) *SS36076-GAL4* expression of GFP labels hIII2 and hI2 motor neurons.

(F and G) *SS41075*-GAL4 labels the hDVM (F) and hI1 motor neurons (G). Magenta shows phalloidin staining of muscles.

Scale bars: 50 μm (A–D) and 25 μm (E–G). See also Figure S2.

modulate the number of active mechanoreceptors at the base of the wing. However, we also measured changes in the terminals of the haltere afferents during presentation of visual motion. These observed changes in haltere afferent activity occurred in the absence of mechanical rotations, i.e., no Coriolis forces acted upon the haltere during our experiments because the body was rigidly fixed. Thus, we interpret the modulation of haltere afferents as resulting from the changes in the activity of haltere steering muscles in response to visual motion (Figure 1). Unfortunately, field-specific driver lines do not exist for either the wing or haltere campaniforms, thus we cannot easily determine which of the many sensilla fields are recruited by the descending visual input. The recruitment of additional campaniforms might come about either through direct alterations in haltere kinematics [16] or via more subtle mechanical changes at the base that regulate the sensitivity of the sensilla without changing the overall motion of the haltere.

If flies modulate mechanosensory input from the haltere to regulate wing motion via descending commands to the haltere motor system, then direct activation of the haltere steering muscles should alter the firing pattern of wing steering muscles. We explicitly tested the capacity for the haltere steering muscles to influence wing steering muscle activity by expressing CsChrimson in haltere steering muscle motor neurons using two different split-GAL4 lines (Figures 3A–3D). *SS36076* (Figures 3A and 3B) targets the motor neurons of haltere muscles hI2

and hIII2 (Figure 3E) as well as a motor neuron of wTP1, the first tergopleural muscle of the wing; whereas *SS41075* (Figures 3C and 3D) targets the motor neurons of haltere muscles hDVM and hI1 (Figures 3F and 3G) along with a motor neuron of a wDVM, a dorso-ventral power muscle of the wing. A recent study demonstrated that the wing steering muscles of *Drosophila* are stratified into two physiological classes [22]: tonic muscles that fire once per wingstroke at specific phases in the stroke cycle and phasic muscles that are recruited in short bursts to execute large changes in wing motion. To examine the influence of the haltere steering muscles on both muscle classes, we recorded from the first basalar wing muscle (wB1), which is tonically active, and the large second basalar wing muscle (wB2), which is phasically active, in separate experiments using sharp tungsten electrodes (Figure 4A) in the absence of any visual stimuli. Without optogenetic activation of either driver line, the wB1 fired one spike per cycle near the upstroke-to-downstroke transition, whereas wB2 was quiescent except for occasional bursts, which is consistent with prior studies [2, 31]. Optogenetic activation of hI2 and hIII2 resulted in phase-delayed firing in wB1 (Figures 4B and 4C). In contrast, optogenetic activation of the hDVM and hI1 resulted in phase-advanced firing of wB1 activity accompanied by recruitment of wB2 (Figures 4D–4G).

Because each of the two driver lines we used to activate haltere motor neurons also targeted a wing muscle, we performed control experiments to test whether the changes in phase and recruitment we recorded could have been due to activation of either wDVM or wTP1. To test the potential influence of wDVM activation, we repeated our experiments using the *SS43980-GAL4* driver line, which targets all six wDVM motor neurons (Figures S2A–S2C). However, optogenetic activation of wDVM motor neurons had no effect on wB1 firing phase or wB2 recruitment (Figure S2D). To test the potential influence of wTP1 activation, we drove expression of CsChrimson using *tp1-SG*, which targets the wTP1 motor neuron [32]; however,
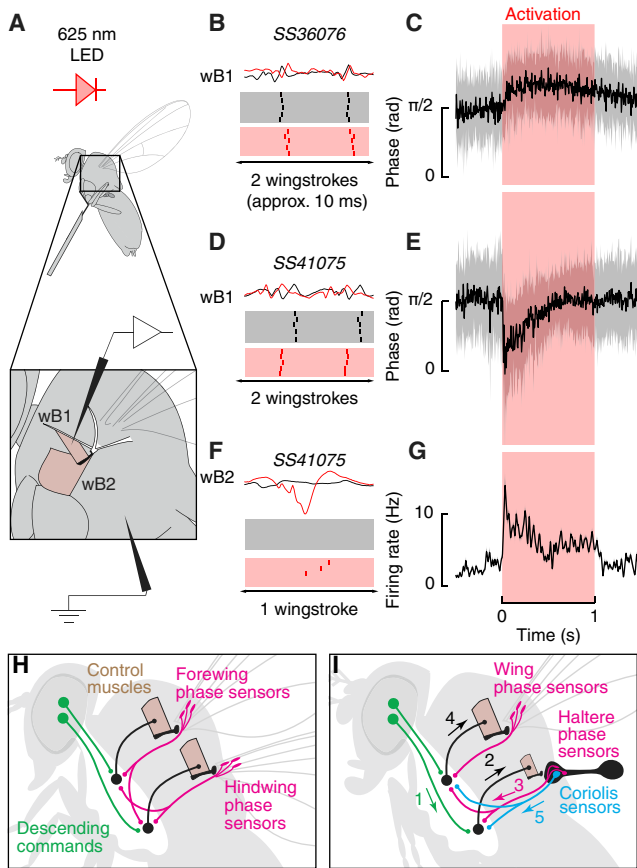
Figure 4. Activation of the Haltere Muscles Is Correlated with Phase Shifts and Recruitment of the Wing Steering System

(A) Schematic of setup used to activate haltere steering motor neurons and simultaneously record wing steering muscle activity during tethered flight. Inset: anatomical locations of the first and second basalar wing steering muscles.

(B) Example muscle action potentials (top) of wB1 before (black) and after (red) optogenetic activation of *SS36076-GAL4*, which targets the motor neurons of hIII2 and hI2. Bottom: raster plots of wB1 firing during the ten wingstrokes 50 ms before optogenetic activation and the first ten wingstrokes after 50 ms of activation.

(C) Instantaneous phase of wB1 in response to *SS36076-GAL4* activation, which targets the motor neurons of hDVM and hI1. Data shown represent circular mean ± circular STD; n = 10.

(D) wB1 activity before and after optogenetic activation of *SS41075-GAL4*.

(E) Same as (C) for *SS41075-GAL4*; n = 7.

(F) wB2 recruitment after *SS41075-GAL4* activation.

(G) Instantaneous wB2 firing rate during *SS41075-GAL4* activation. Data shown represent mean ± 95% CI; n = 6 flies.

(H) Proposed scenario that led to the evolution of the halteres. The ancestor of flies possessed four wings and relied on wingbeat synchronous mechanosensory input from the fore and hindwings along with descending visual commands to structure the timing of motor output.

(I) The transformation of the hindwings into halteres provided flies with a clock signal that was not contaminated by the production of aerodynamic forces. Visual input to the haltere muscles (1) leads to activation of control muscles (2) that recruit additional campaniform sensilla each stroke (3). As a result, the firing phase of tonic wing steering muscles changes along with recruitment of phasic muscles (4). In our scheme, the Coriolis function of the haltere represents a separate sensory pathway (5).

See also Figure S2.

optogenetic activation of the wTP1 motor neuron had no effect on wB1 firing phase (Figure S2E). We also tested for the influence of the CsChrimson activation light on wing steering muscle activity by performing control experiments using a split-GAL4 empty vector driver line crossed with *UAS-CsChrimson* but saw no effect on the wing steering muscles we recorded (Figure S2F).

Although the haltere is commonly described as a gyroscope, the structure is better interpreted as a multifunctional sensory organ. One role of the haltere is to provide phasic, clock-like drive to the wing steering motor neurons at stroke frequency via campaniform fields that are sensitive to the large inertial forces generated by haltere oscillation [7]. Another role is to function as a gyroscope to encode angular rotation of the body during flight [10]. These roles are not incompatible, because the halteres possess multiple arrays of campaniform sensilla that differ in their directional sensitivity to the strains acting on the structure as it beats back and forth during flight [10]. For example, the campaniforms embedded on the haltere's stalk, dorsal field 3 (dF3) and ventral field 2 (vF2), are oriented along the structure's long axis, suggesting that these sensors detect the large inertial strains within the stroke plane as the haltere beats up and down [10, 11, 33–35]. By contrast, the campaniforms in dorsal field 2 (dF2) are arranged at an orientation that would make them most sensitive to shear strains resulting from the Coriolis forces that act laterally to the stroke plane when the fly's body rotates [10, 11]. This functional stratification invites the question: which classes of campaniform sensilla are regulated by the haltere muscles?

The original control loop hypothesis of Chan et al. [16] posited that the descending commands recruit the Coriolis-sensitive sensilla. In this scheme, visual motion induces steering by, in essence, generating virtual perturbations that activate the reflex loop consisting of dF2 campaniforms and wing steering motor neurons. Prior work in dissected, non-flying blowflies indicates that campaniform sensilla in dF2 make direct, monosynaptic connections with the motor neuron of the ipsilateral wB1 via a mixed chemical-electrical synapse [8, 9, 36]. Furthermore, stimulation of the haltere nerve can drive a phase advance of a wB1 motor neuron that is entrained by repetitive stimulation of the wing nerve [8, 9]. These observations are compatible with the changes in firing phase of wB1 we observed during optogenetic activation of haltere motor neurons (Figure 4). However, it is also possible that the haltere muscles act to recruit campaniforms of the Coriolis-insensitive fields (e.g., dF3 and vF2), thus altering the phasic drive to the steering motor neurons without changing the activity of sensilla within dF2. Haltere afferents in *Drosophila* also directly project to wB1, although it is unclear which field provides this input [37]. In addition, single-unit recordings in crane flies and flesh flies show that different campaniforms are active at different phases of the haltere stroke cycle [30, 38]. By changing the relative strength of recruitment among fields, the haltere muscles might act to bias the wing motor neurons to fire at different phase points within the stroke cycle. It is also possible that there is no simple dichotomy, but rather the haltere steering muscles can modulate the activity of all the campaniform sensilla, including those sensitive to Coriolis forces and those that encode the basic oscillatory motion. Unfortunately, because there are as of yet no driver lines that

specifically label the different campaniform fields at the base of the haltere, we were not able to test among these alternatives.

Irrespective of which campaniform fields are involved, our findings provide an example of how nervous systems integrate sensory input from multiple modalities. To regulate the phase of steering muscles, flies must combine the relatively slow descending feedback from the visual or olfactory system with fast wingbeat-synchronous input from the wing. Previous mathematical models suggest that this integration might occur at the level of wing steering motor neurons [39, 40], and indeed, some descending neurons project directly to the dorsal flight neuropil of the 2nd thoracic segment [41]. Additionally, previous behavioral work indicates that flies are able to execute tethered flight turns without their halteres; however, the steering responses of haltere-less flies to wide-field motion are diminished compared to intact controls [42]. Furthermore, other descending cells project to the 3rd thoracic segment, where the dendrites of haltere motor neurons reside [41]. Thus, our results indicate an alternative pathway through which descending visual input is transformed into phase-coded steering commands via recruitment of haltere mechanoreceptors. Haltere afferents also project to neck motor neurons used for gaze stabilization [43, 44]. Thus, not only can the visual system control the gain of feedback from the halteres, the relationship is reciprocal.

Our results provide further support for a parsimonious scenario by which the haltere evolved from an aerodynamically functional hindwing (Figures 4H and 4I) [16]. In four-winged insects, such as locusts, mechanoreceptors on both sets of wings provide important phasic feedback to the pattern generator circuits that drive the wing motor neurons [45, 46]. In flies, the precise activation phase of the steering muscles relies on wingbeat-synchronous mechanosensory feedback, and there is no evidence that a central pattern generator is involved in generating the phase-locked firing patterns [7, 9, 47]. Although sensory feedback from wing mechanoreceptors may help set the firing phase of steering muscles, any potential for the wings to act as a controllable clock is complicated by the fact that wings experience both aerodynamic and inertial forces as they flap. Although recent evidence suggests that the wings of larger insects might disambiguate these forces during rotational perturbations [48], the wing mechanoreceptors can never provide as clean a clock signal as the mechanoreceptors on a haltere. As the fly adjusts wing motion during a maneuver, the resulting changes in the production of aerodynamic forces will alter the firing of mechanoreceptors at the base of the wing. By reducing the hindwing to a tiny structure that plays no aerodynamic role, flies would have gained an independent clock providing phasic signals that remain constant during flight (Figure 4I). The strong connection between hind wing mechanoreceptors and forewing muscles found in four-winged insects [49] provides a likely pre-adaptation for the specialized circuit that we have described. The advantage of this aerodynamically independent timing circuit may have been the principle selective pressure driving the evolution of the halteres, whereas the gyroscopic function of the haltere may represent a subsequent modification when one campaniform field (dorsal field 2) became specialized for the detection of the very small lateral strains caused by Coriolis forces [10]. Much like the functional stratification of the wing steering system, the transformation of

the hindwing into an adjustable clock that can also detect body rotations allows flies to execute rapid aerial maneuvers while remaining sensitive to external perturbations. Whereas the separation between controlling stabilization reflexes and voluntary maneuvers may be achieved by different activation thresholds in the case of the wing steering muscles [22], the directional sensitivity of the different campaniform arrays on the haltere may enable its multifunctional capacity. The increased agility of flies relative to other flying insects possibly allowed them to infiltrate many ecological niches, contributing to their success as an order [50].

STAR★METHODS

Detailed methods are provided in the online version of this paper and include the following:

- KEY RESOURCES TABLE
- LEAD CONTACT AND MATERIALS AVAILABILITY
- EXPERIMENTAL MODEL AND SUBJECT DETAILS
- METHOD DETAILS
  - Flight arenas and visual stimuli
  - Flight behavior
  - Functional imaging
  - Optogenetic activation of haltere steering muscles
  - Histology and confocal microscopy
- QUANTIFICATION AND STATISTICAL ANALYSIS
  - Determining wing steering muscle phase of activation and spike rate
- DATA AND CODE AVAILABILITY

AUTHOR CONTRIBUTIONS

Conceptualization, B.H.D. and M.H.D.; Methodology, B.H.D., A.M.d.S., A.H., and M.H.D.; Investigation, B.H.D., A.M.d.S., and A.H.; Writing – Original Draft, B.H.D. and M.H.D.; Writing – Review & Editing, B.H.D. and M.H.D.; Funding Acquisition, B.H.D. and M.H.D.; Resources, M.H.D.; Supervision, M.H.D.

DECLARATION OF INTERESTS

The authors declare no competing interests.

REFERENCES

1. Nachtigall, W., and Wilson, D.M. (1967). Neuro-muscular control of dipteran flight. J. Exp. Biol. *47*, 77–97.

2. Heide, G., and Götz, K.G. (1996). Optomotor control of course and altitude in *Drosophila melanogaster* is correlated with distinct activities of at least three pairs of flight steering muscles. J. Exp. Biol. *199*, 1711–1726.

3. Balint, C.N., and Dickinson, M.H. (2001). The correlation between wing kinematics and steering muscle activity in the blowfly *Calliphora vicina*. J. Exp. Biol. *204*, 4213–4226.

4. Josephson, R.K. (1985). Mechanical power output from striated muscle during cyclic contraction. J. Exp. Biol. *114*, 493–512.

5. Tu, M., and Dickinson, M. (1994). Modulation of negative work output from a steering muscle of the blowfly *Calliphora vicina*. J. Exp. Biol. *192*, 207–224.

6. Lehmann, F.O., and Götz, K.G. (1996). Activation phase ensures kinematic efficacy in flight-steering muscles of *Drosophila melanogaster*. J. Comp. Physiol. A Neuroethol. Sens. Neural Behav. Physiol. *179*, 311–322.

7. Heide, G. (1983). Neural mechanisms of flight control in Diptera. In BIONA Report 2, W. Nachtigall, ed. (Gustav Fischer Verlag), pp. 35–52.

8. Fayyazuddin, A., and Dickinson, M.H. (1996). Haltere afferents provide direct, electrotonic input to a steering motor neuron in the blowfly, *Calliphora*. J. Neurosci. *16*, 5225–5232.

9. Fayyazuddin, A., and Dickinson, M.H. (1999). Convergent mechanosensory input structures the firing phase of a steering motor neuron in the blowfly, *Calliphora*. J. Neurophysiol. *82*, 1916–1926.

10. Pringle, J.W.S. (1948). The gyroscopic mechanism of the halteres of Diptera. Philos. Trans. Royal Soc. B *233*, 347–384.

11. Fraenkel, G., and Pringle, J.W.S. (1938). Biological sciences: halteres of flies as gyroscopic organs of equilibrium. Nature *141*, 919–920.

12. Hengstenberg, R. (1988). Mechanosensory control of compensatory head roll during flight in the blowfly *Calliphora erythrocephala* Meig. J. Comp. Physiol. A *163*, 151–165.

13. Nalbach, G. (1993). The halteres of the blowfly *Calliphora*. I. Kinematics and dynamics. J. Comp. Physiol. A *173*, 293–300.

14. Nalbach, G., and Hengstenberg, R. (1994). The halteres of the blowfly *Calliphora*. II. Three-dimensional organization of compensatory reactions to real and simulated rotations. J. Comp. Physiol. A *175*, 695–708.

15. Dickinson, M.H. (1999). Haltere-mediated equilibrium reflexes of the fruit fly, *Drosophila melanogaster*. Philos. Trans. R. Soc. Lond. B Biol. Sci. *354*, 903–916.

16. Chan, W.P., Prete, F., and Dickinson, M.H. (1998). Visual input to the efferent control system of a fly's "gyroscope". Science *280*, 289–292.

17. Cole, E.S., and Palka, J. (1982). The pattern of campaniform sensilla on the wing and haltere of *Drosophila melanogaster* and several of its homeotic mutants. J. Embryol. Exp. Morphol. *71*, 41–61.

18. Bonhag, P.F. (1949). Thoracic mechanism of the adult horsefly: Diptera, Tabanidae (Cornell University Agricultural Experiment Station), pp. 3–39.

19. Mickoleit, G. (1962). Die Thoraxmuskulatur von *Tipula vernalis* Meigen. Ein Beitrag zur vergleichenden Anatomie des Dipterenthorax. Zool. Jb. Anat. Bd. *80*, 213–244.

20. Ulrich, H. (1984). Skelett und Muskulatur des Thorax von *Microphor holosericeus* (Meigen) (Diptera, Empidoidea). Bonn. Zool. Beitr. *35*, 351–398.

21. Pringle, J.W.S. (1949). The excitation and contraction of the flight muscles of insects. J. Physiol. *108*, 226–232.

22. Lindsay, T., Sustar, A., and Dickinson, M. (2017). The function and organization of the motor system controlling flight maneuvers in flies. Curr. Biol. *27*, 345–358.

23. Götz, K.G. (1968). Flight control in *Drosophila* by visual perception of motion. Kybernetik *4*, 199–208.

24. Suver, M.P., Huda, A., Iwasaki, N., Safarik, S., and Dickinson, M.H. (2016). An array of descending visual interneurons encoding self-motion in *Drosophila*. J. Neurosci. *36*, 11768–11780.

25. Palka, J., Lawrence, P.A., and Hart, H.S. (1979). Neural projection patterns from homeotic tissue of *Drosophila* studied in bithorax mutants and mosaics. Dev. Biol. *69*, 549–575.

26. Tsubouchi, A., Yano, T., Yokoyama, T.K., Murtin, C., Otsuna, H., and Ito, K. (2017). Topological and modality-specific representation of somatosensory information in the fly brain. Science *358*, 615–623.

27. Palka, J., Malone, M.A., Ellison, R.L., and Wigston, D.J. (1986). Central projections of identified *Drosophila* sensory neurons in relation to their time of development. J. Neurosci. *6*, 1822–1830.

28. Dickinson, M.H. (1990). Comparison of encoding properties of campaniform sensilla on the fly wing. J. Exp. Biol. *151*, 245–261.

29. Fox, J.L., and Daniel, T.L. (2008). A neural basis for gyroscopic force measurement in the halteres of *Holorusia*. J. Comp. Physiol. A Neuroethol. Sens. Neural Behav. Physiol. *194*, 887–897.

30. Fox, J.L., Fairhall, A.L., and Daniel, T.L. (2010). Encoding properties of haltere neurons enable motion feature detection in a biological gyroscope. Proc. Natl. Acad. Sci. USA *107*, 3840–3845.

31. Tu, M.S., and Dickinson, M.H. (1996). The control of wing kinematics by two steering muscles of the blowfly (*Calliphora vicina*). J. Comp. Physiol. A Neuroethol. Sens. Neural Behav. Physiol. *178*, 813–830.

32. O'Sullivan, A., Lindsay, T., Prudnikova, A., Erdi, B., Dickinson, M., and von Philipsborn, A.C. (2018). Multifunctional wing motor control of song and flight. Curr. Biol. *28*, 2705–2717.e4.

33. Smith, D.S. (1969). The fine structure of haltere sensilla in the blowfly *Calliphora erythrocephala* (Meig.), with scanning electron microscopic observations on the haltere surface. Tissue Cell *1*, 443–484.

34. Chevalier, R.L. (1969). The fine structure of campaniform sensilla on the halteres of *Drosophila melanogaster*. J. Morphol. *128*, 443–463.

35. Agrawal, S., Grimaldi, D., and Fox, J.L. (2017). Haltere morphology and campaniform sensilla arrangement across Diptera. Arthropod Struct. Dev. *46*, 215–229.

36. Chan, W.P., and Dickinson, M.H. (1996). Position-specific central projections of mechanosensory neurons on the haltere of the blow fly, *Calliphora vicina*. J. Comp. Neurol. *369*, 405–418.

37. Trimarchi, J.R., and Murphey, R.K. (1997). The *shaking-B²* mutation disrupts electrical synapses in a flight circuit in adult *Drosophila*. J. Neurosci. *17*, 4700–4710.

38. Yarger, A.M., and Fox, J.L. (2018). Single mechanosensory neurons encode lateral displacements using precise spike timing and thresholds. Proc. Biol. Sci. *285*, 20181759.

39. Bartussek, J., and Lehmann, F.O. (2016). Proprioceptive feedback determines visuomotor gain in *Drosophila*. R. Soc. Open Sci. *3*, 150562.

40. Bartussek, J., and Lehmann, F.O. (2018). Sensory processing by motoneurons: a numerical model for low-level flight control in flies. J. R. Soc. Interface *15*, 20180408.

41. Namiki, S., Dickinson, M.H., Wong, A.M., Korff, W., and Card, G.M. (2018). The functional organization of descending sensory-motor pathways in *Drosophila*. eLife *7*, e34272.

42. Mureli, S., and Fox, J.L. (2015). Haltere mechanosensory influence on tethered flight behavior in *Drosophila*. J. Exp. Biol. *218*, 2528–2537.

43. Strausfeld, N.J., and Seyan, H.S. (1985). Convergence of visual, haltere, and prosternal inputs at neck motor neurons of *Calliphora erythrocephala*. Cell Tissue Res. *240*, 601–615.

44. Huston, S.J., and Krapp, H.G. (2009). Nonlinear integration of visual and haltere inputs in fly neck motor neurons. J. Neurosci. *29*, 13097–13105.

45. Gettrup, E. (1965). Sensory mechanisms in locomotion: the campaniform sensilla of the insect wing and their function during flight. Cold Spring Harb. Symp. Quant. Biol. *30*, 615–622.

46. Gettrup, E. (1966). Sensory regulation of wing twisting in locusts. J. Exp. Biol. *44*, 1–16.

47. Heide, G. (1979). Proprioceptive feedback dominates the central oscillator in the patterning of the flight motoneuron output in *Tipula* (Diptera). J. Comp. Physiol. *134*, 177–189.

48. Eberle, A.L., Dickerson, B.H., Reinhall, P.G., and Daniel, T.L. (2015). A new twist on gyroscopic sensing: body rotations lead to torsion in flapping, flexing insect wings. J. R. Soc. Interface *12*, 20141088.

49. Wolf, H. (1993). The locust tegula: significance for flight rhythm generation, wing movement control and aerodynamic force production. J. Exp. Biol. *182*, 229–253.

50. Grimaldi, D., and Engel, M.S. (2005). Evolution of the Insects (Cambridge University Press).

51. Hampel, S., Franconville, R., Simpson, J.H., and Seeds, A.M. (2015). A neural command circuit for grooming movement control. eLife *4*, e08758.

52. Weir, P.T., Henze, M.J., Bleul, C., Baumann-Klausener, F., Labhart, T., and Dickinson, M.H. (2016). Anatomical reconstruction and functional imaging reveal an ordered array of skylight polarization detectors in *Drosophila*. J. Neurosci. *36*, 5397–5404.

53. Reiser, M.B., and Dickinson, M.H. (2008). A modular display system for insect behavioral neuroscience. J. Neurosci. Methods *167*, 127–139.

54. Götz, K.G. (1987). Course-control, metabolism and wing interference during ultralong tethered flight in *Drosophila melanogaster*. J. Exp. Biol. *128*, 35–46.

STAR★METHODS

KEY RESOURCES TABLE

REAGENT or RESOURCE	SOURCE	IDENTIFIER
Antibodies		
Rabbit polyclonal anti-GFP	ThermoFisher Scientific	A21311; RRID: AB_221477
Alexa Fluor 488 goat anti-rabbit	ThermoFisher Scientific	A11008; RRID: AB_143165
Alexa Fluor 633 goat anti-mouse	ThermoFisher Scientific	A21050; RRID: AB_2535718
Alexa Fluor 568 phalloidin	ThermoFisher Scientific	A12380; RRID: AB_2759224
Mouse mAb anti-Bruchpilot (nc82)	Developmental Studies Hybridoma Bank	nc82; RRID: AB_2314866
Chemicals, Peptides, and Recombinant Proteins		
All-trans-retinal	Sigma-Aldrich	R2500
Deposited Data		
Raw and analyzed data	This paper	https://doi.org/10.17632/kp9hbmxn47.1
Experimental Models: Organisms/Strains		
D. melanogaster: DB331-GAL4	FlyBase	FBti0115113
D. melanogaster: GMR12C07-GAL4	Bloomington Drosophila Stock Center	RRID: BDSC_48496
D. melanogaster: GMR22H05-GAL4	Bloomington Drosophila Stock Center	RRID: BDSC_49002
D. melanogaster: ; P{y$^{+t7.7}$ w^{+mC} = 20XUAS-IVS-GCaMP6f}attP40	Bloomington Drosophila Stock Center	RRID:BDSC_42747
D. melanogaster: ; P{y$^{+t7.7}$ w^{+mC} = 10XUAS-IVS-myr::tdTomato}attP2	Bloomington Drosophila Stock Center	RRID:BDSC_32221
D. melanogaster: ;UAS-GCaMP6f; UAS-tdTomato	Constructed from above two lines	N/A
D. melanogaster: SS36076-SplitGAL4	Gift from G. Card, E. Ehrhardt, and W. Korff	N/A
D. melanogaster: SS41075-SplitGAL4	Gift from G. Card, E. Ehrhardt, and W. Korff	N/A
D. melanogaster: SS43980-SplitGAL4	Gift from G. Card, E. Ehrhardt, and W. Korff	N/A
D. melanogaster: tp1-SG	Gift from A. von Philipsborn [32]	N/A
D. melanogaster: Empty-SplitGAL4(; P{w[+mC] = BP-p65ADzpUw}attP40 and P{w[+mC] = BP-ZpGal4DBDUw}attP2)	Gift from J. Simpson [51]	N/A
D. melanogaster: ; P{y$^{+t7.7}$ w^{+mC} = 20XUAS-IVS-CsChrimson.mVenus}attP2	Bloomington Drosophila Stock Center	RRID:BDSC_55136
Software and Algorithms		
Python 2.7	https://www.python.org/	RRID: SCR_008394
Matplotlib	https://matplotlib.org/	RRID: SCR_008624
FIJI	NIH (https://fiji.sc/)	RRID:SCR_002285

LEAD CONTACT AND MATERIALS AVAILABILITY

This study did not generate new unique genetic reagents. Further information should be directed to Lead Contact, Michael Dickinson (flyman@caltech.edu).

EXPERIMENTAL MODEL AND SUBJECT DETAILS

All flies used in this study were 2-to-11 day old females. For imaging experiments, we raised flies on standard cornmeal medium at 25°C on a 12:12 hour light/dark cycle. For CsChrimson activation experiments, we raised the parents and progeny in continuous darkness. We supplemented the food for the parents with 100 μL of 100 mM all-trans retinal, and 200 μL of the same concentration for the progeny.

We expressed GCaMP6f and tdTomato in the haltere afferents by crossing *DB331-GAL4* to +[HCS]; P{20XUAS-IVS-GCaMP6f}attP40; P{w[+mC] = UAS-tdTom.S}3. To image from the wing afferents, we crossed w[1118];+; P{y[+t7.7] w[+mC] = GMR12C07-GAL4}attP2 with +[HCS]; P{20XUAS-IVS-GCaMP6f}attP40; P{w[+mC] = UAS-tdTom.S}3. To prepare flies for 2-photon imaging,

we chilled them to 4°C and removed the first two pairs of legs and the tibia and tarsi of the metathoracic legs. We then mounted the flies to custom-built stages using UV-cured glue [52]. These stages allow flies to flap their wings while simultaneously allowing access to the back of the head capsule for physiology. Before each experiment, we dissected a small hole where the base of the head meets the neck with a hypodermic needle in saline and severed the esophagus. We perfused the brain with 19°C saline during experiments.

We crossed w[1118];+; P{y[+t7.7] w[+mC] = GMR22H05-GAL4}attP2 with +[HCS]; P{20XUAS-IVS-GCaMP6f}attP40;+ to express GCaMP6f in the haltere steering muscles. The haltere muscles are located at the posterior part of the thorax, dorsal of the posterior spiracle, and are thus subject to substantial motion artifact during tethered flight. To help stabilize our images, we removed the first two pairs of legs and fixed the flies ventrally with UV-cured glue to the tip of a tungsten pin between the femur of the prothoracic legs and the coxae of the mesothoracic legs.

To express CsChrimson in the haltere steering mucles, we crossed either *SS36076-SplitGAL4* or *SS41075-SplitGAL4* with w[*];+; P{20XUAS-IVS-CsChrimson.mVenus}attP2. For activation controls, we crossed either *SS43980-SplitGAL4,* +; P{w[+mC] = BP-p65ADzpUw}attP40; P{w[+mC] = BP-ZpGal4DBDUw}attP2 [51], or *tp1-SG* to CsChrimson. We tethered flies as in our muscle imaging experiments, but after removing all three pairs of legs.

METHOD DETAILS

Flight arenas and visual stimuli

For imaging of the haltere steering muscles, we placed flies in the center of an arena composed of blue light-emitting diodes (LEDs; 470 nm peak wavelength) as described previously [53]. The arena spanned ± 60° in elevation from the fly's horizon (32 pixels) and 270° around its azimuth (72 pixels; 3.75°/pixel). To accommodate the imaging objective, there was a 90° gap in azimuth on the left side of the arena. We placed one layer of blue filter to prevent light from the display from leaking into the camera used for imaging GCaMP activity.

All visual stimuli consisted of wide-field, random dot starfields. To test rotational tuning about the yaw-roll and pitch-roll axes, we altered the center of rotation in 30° increments. To test tuning in the yaw-roll plane, we shifted the stimulus from the vertical body axis to the longitudinal axis. To test tuning in the pitch-roll plane, we shifted the stimulus from the longitudinal axis to the transverse body axis. We displayed patterns in a random blocks for a duration of 3 s each, five repetitions for each stimulus. To promote flight, we presented flies with a dark stripe on a bright background under closed-loop conditions for 5 s between each trial.

For 2-photon imaging, we placed flies within a similar blue LED that spanned ± 108° (96 pixels) in azimuth around the center of the fly and ± 32° (32 pixels) in elevation (2.25°/pixel). We used six layers of filter (one Rosco #59 indigo, two #39 sangria, two #4390 cyan) to prevent saturation of the photomultiplier tubes. Each fly experienced five repetitions of each stimulus in a random order for a duration of 3 s. Rotational patterns for all experiments simulated motion at an angular velocity of 180°s^{-1}. Between stimuli, the entire LED arena was dark for 2 s. The pattern then appeared and was still for 1 s before stimulus presentation.

Flight behavior

To track steering behavior during muscle imaging experiments, we placed flies within an optoelectronic wingbeat analyzer [54]. The moving wings cast shadows onto an optical sensor that converts instantaneous wingbeat amplitude into a voltage signal. We acquired wingbeat amplitude data at 2 kHz using a Digidata 1440A amplifier (Molecular Devices). In cases where flies stopped flying, we softly blew on them to resume behavior. To track steering during imaging of the haltere terminals, we illuminated each fly with four IR LEDs via optical fibers while a camera recorded each fly's behavior at 32 Hz. A custom machine vision algorithm computed and saved the left and right wingstroke amplitudes [24].

Functional imaging

Our method for imaging haltere muscle activity was similar to that described for recording wing muscle activity [22]. We imaged the haltere muscles with a 50x, 0.55 NA objective (Mitutoyo) mounted to a Nikon Eclipse FN1 epifluorescence microscope. We placed the fly, flight arena, and wing beat analyzer sideways to access the muscles. We excited GCaMP6f within the muscles with continuous 470 nm light (M470L3, Thorlabs), and collected images with a QIClick camera (QImaging) after they were band-passed filtered by an ET535/50 m emission filter (Chroma Technology). The amplifier we used to collect wingbeat amplitude data sent a TTL pulse to an Arduino Due, which triggered the camera at a phase of 0.75 relative to the upstroke of the wings. We collected TIFF stacks at an exposure time of 33 ms using µManager.

To image the haltere and wing afferent axon terminals, we used a Nikon 40x NIR Apo water immersion lens (0.8 NA) with a ThorLabs 2-photon microscope (Bergamo II series B206) at an excitation wavelength of 930 nm provided by a MaiTai DeepSee Ti:Sapphire laser (Spectra-Physics). We recorded images at a resolution of 47.74 × 15.91 µm or 41.77 × 13.92 µm for the haltere and wing afferent terminals, respectively. We imaged calcium activity at a frame rate of 30.8 Hz and a laser power (measured at the back aperture of the objective) of 5.6-7.4 mW.

Optogenetic activation of haltere steering muscles

We excited the haltere steering muscles during tethered flight using a 1 s pulse of 625 nm light (M625F2, Thorlabs) at a stimulus intensity of 20 mA. We used electrolytically sharpened tungsten electrodes to record from the steering muscles through the cuticle. We identified both wB1 and wB2 through a combination of anatomical location and their response properties in flight [2, 6, 7]. The wB1

muscle typically fires a single muscle action potential per wingstroke at a characteristic phase in the stroke cycle, approximately the transition from upstroke to downstroke. The wB2 muscle is typically silent during flight, only firing in short bursts. To confirm that we placed our recording electrode in the proper location, we gently blew on the fly during flight. A short burst of spikes in response to this stimulus satisfied our criteria that we were recording wB2 and we then proceeded with our stimulus protocol. We performed all experiments in the dark. We recorded the raw wingbeat signal, wingbeat amplitude, and electrophysiological data at 20 kHz using a Digidata 1440A amplifier and AxoScope.

Histology and confocal microscopy

We dissected brains and thoracic ganglia in 4% paraformaldehyde in PBS and then washed them in PBS-TX. We stained the tissue overnight at 4°C with 1:10 mouse anti-nc82 and 1:1000 rabbit anti-GFP in PBS-TX. Then, we washed the brains in PBS-TX and applied a secondary antibody stain consisting of 1:250 goat anti-mouse AlexaFluor 633 and 1:250 goat anti-rabbit AlexaFluor 488 in PBS-TX either overnight at 4°C or for three hours at room temperature. To prepare the haltere muscles for confocal imaging, we hemisected flies frozen in O.C.T. medium (Electron Microscopy Sciences no. 62550-01) along the midline and transferred them into 4% paraformaldehyde in PBS. We then stained the muscles for 7-10 days at 4°C with 1:50 AlexaFluor 568 phalloidin (Invitrogen no. A12380) and 1:100 rabbit anti-GFP AlexaFluor 488 conjugate (Invitrogen no. A21311). After staining, we cleared the tissue in SeeDB. We collected all confocal image stacks on a Leica TCS SP8 with a 40x objective at a resolution of 1024x1024 pixels. We performed at least ten hemisections for each driver line.

QUANTIFICATION AND STATISTICAL ANALYSIS

We analyzed our imaging and flight behavior data using custom scripts written in Python. For the muscle imaging experiments, we rigidly registered each image to the image of the muscles at the middle of the experiment. We then fit these images to a model of the haltere muscles. The model consisted of the contours of the identified haltere muscles taken at a magnification of 40x. We used an affine transformation to warp each image stack to this model and thus all images into a common reference frame. We used this same muscle model as regions of interest (ROIs) for our image stacks, separately grouping the basalares and axillaries to compute mean fluorescence.

After segmenting our images, we computed the change in GCaMP6f fluorescence F_t for each time point. For each muscle group, we computed the mean baseline fluorescence F_0 for 0.5 s prior to stimulus motion before computing $(F_t-F_0)/F_0$, which we term "ΔF/F."

For our experiments imaging the wing and haltere axon terminals, we first rigidly registered each frame from the tdTomato channel by finding the peak of the cross-correlation between it and the mean image. Next, we registered the GCaMP6f channel to the tdTomato channel. We then corrected for any movement out of the focal plane by dividing the pixel intensities of the GCaMP6f channel by those of the tdTomato signal. To define our ROI, we found the brightest 50% of all pixels in the mean image of the registered GCaMP6f channel, and used the dimmest 50% as our background. The difference between the mean fluorescence in the ROI and background for each image is defined as F_t. To calculate the change in fluorescence for each stimulus, we computed F_0 for the 1 s prior to visual motion.

To condition our wingbeat amplitude signals, we calculated the mean wingstroke angle or voltage of the left wingbeat amplitude detector over the same 1 s or 0.5 s interval before stimulus motion as the fluorescence signal. We then subtracted this baseline from the signal during image motion. To calculate population responses to each visual stimulus, we calculated each fly's mean response to a given pattern to construct an individual mean. We then pooled these individual means to compute the population average. We constructed 95% confidence intervals by resampling the population average 1,000 times with replacement from the individual means. To construct tuning curves, we summed each fly's individual mean fluorescence and wingbeat amplitude signals during the 3 s stimulus period for each stimulus direction.

Determining wing steering muscle phase of activation and spike rate

To calculate when in the stroke cycle wB1 and wB2 fired, we first used a narrow 4th order band-pass Butterworth filter (100 to 300 Hz) on the raw wingbeat signal. We then performed a Hilbert transform on this signal to determine the instantaneous phase of the transition from upstroke to downstroke. Using the timestamps of the identified muscle action potentials, we then found the instantaneous wB1 phase throughout the experiment. To calculate wB2 spike rate, we convolved the timestamps of identified spikes with a Gaussian filter (50 ms width, 7.5 ms STD). We constructed 95% confidence intervals of wB2 spike rate by resampling the population average 500 times with replacement from the individual means. Throughout the paper, n refers to the number of flies.

DATA AND CODE AVAILABILITY

The data from this manuscript are published on Mendeley Data at: https://doi.org/10.17632/kp9hbmxn47.1